Vaccine: X 20 (2024) 100543

Contents lists available at ScienceDirect

Vaccine: X

journal homepage: www.elsevier.com/locate/jvacx

Influenza virus strains expressing SARS-CoV-2 receptor binding domain protein confer immunity in K18-hACE2 mice

Nathaniel A. Rader [a,b,1], Katherine S. Lee [a,b,1], Andrea N. Loes [c,d], Olivia A. Miller-Stump [a,b], Melissa Cooper [a,b], Ting Y. Wong [a,b], Dylan T. Boehm [a,b], Mariette Barbier [a,b], Justin R. Bevere [a,b], F. Heath Damron [a,b,*]

[a] Department of Microbiology, Immunology, and Cell Biology, West Virginia University, Morgantown, WV, USA
[b] Vaccine Development Center at West Virginia University Health Sciences Center, Morgantown, WV, USA
[c] Division of Basic Sciences and Computational Biology Program, Fred Hutchinson Cancer Research Center, Seattle, WA 98109, USA
[d] Howard Hughes Medical Institute, Seattle, WA 98103, USA

ARTICLE INFO

Keywords:
SARS-CoV-2
Delta
Omicron
Influenza virus
Intranasal vaccine
Vaccine

ABSTRACT

Severe acute respiratory syndrome coronavirus 2 (SARS-CoV-2), the causative agent of coronavirus disease (COVID-19), rapidly spread across the globe in 2019. With the emergence of the Omicron variant, COVID-19 shifted into an endemic phase. Given the anticipated rise in cases during the fall and winter seasons, the strategy of implementing seasonal booster vaccines for COVID-19 is becoming increasingly valuable to protect public health. This practice already exists for seasonal influenza vaccines to combat annual influenza seasons. Our goal was to investigate an easily modifiable vaccine platform for seasonal use against SARS-CoV-2. In this study, we evaluated the genetically modified influenza virus ΔNA(RBD) as an intranasal vaccine candidate for COVID-19. This modified virus was engineered to replace the coding sequence for the neuraminidase (NA) protein with a membrane-anchored form of the receptor binding domain (RBD) protein of SARS-CoV-2. We designed experiments to assess the protection of ΔNA(RBD) in K18-hACE2 mice using lethal (Delta) and non-lethal (Omicron) challenge models. Controls of COVID-19 mRNA vaccine and our lab's previously described intranasal virus like particle vaccine were used as comparisons. Immunization with ΔNA(RBD) expressing ancestral RBD elicited high anti-RBD IgG levels in the serum of mice, high anti-RBD IgA in lung tissue, and improved survival after Delta variant challenge. Modifying ΔNA(RBD) to express Omicron variant RBD shifted variant-specific antibody responses and limited viral burden in the lungs of mice after Omicron variant challenge. Overall, this data suggests that ΔNA(RBD) could be an effective intranasal vaccine platform that generates mucosal and systemic immunity towards SARS-CoV-2.

Introduction

Severe acute respiratory syndrome coronavirus 2 (SARS-CoV-2), the causative agent of the corona virus disease of 2019 (COVID-19) pandemic, emerged in 2019 and was marked as an international public health crisis by the World Health Organization (WHO) in early 2020 [1]. Since the first genome sequencing of the SARS-CoV-2 ancestral variant [2] was released in January 2020, multiple variants of concern (VOC) harboring genetic mutations have emerged. Many of these mutations were found in the receptor binding domain (RBD) of the viral spike protein which mediates host cell entry and subsequent infection. Mutations such as N501Y, E484K, and K417N increased the infectivity of early variants such as Alpha, Beta, and Gamma, while simultaneously reducing the protection of antibodies generated previously by either infection or vaccination [3,4]. The Delta variant grew to dominance in 2021 and subsequently acquired several distinctive mutations including E484Q in the spike protein and L452R in RBD [3,5]. These mutations once again increased transmissibility and infectivity, among even the world's vaccinated population, bringing attention to the potential waning protection of ancestral strain-based vaccines against arising

* Corresponding author at: Department of Microbiology, Immunology, and Cell Biology, West Virginia University School of Medicine, 64 Medical Center Drive, HSC North 2105, Morgantown, WV 26506, USA.
E-mail address: fdamron@hsc.wvu.edu (F. Heath Damron).
[1] Authors contributed equally.

https://doi.org/10.1016/j.jvacx.2024.100543
Received 7 May 2024; Accepted 1 August 2024
Available online 3 August 2024

variants of SARS-CoV-2. In December 2021, the Omicron variant emerged and rapidly became the most prevalent strain in the U.S. population [6]. Subvariants within the Omicron lineage have continued to harbor mutations to the spike protein, adding to the 50 estimated mutations identified in initial characterizations of this virus. Over time, these mutations have dramatically altered the protein and its structural similarity to any previous variants, shifting antigenic epitopes further and challenging the protection afforded by antibodies from current SARS-CoV-2 vaccines [3,7–9].

To date, 11 COVID-19 vaccines have been granted emergency use listing (EUL) by the WHO [10]. While these vaccines have been largely effective in reducing morbidity and mortality from SARS-CoV-2 infections, the problem of breakthrough cases in immunized or previously infected individuals remains widely apparent [11–14]. It is appreciated that COVID-19 vaccines do not fully limit transmission of the virus in asymptomatic cases of infection [7,15]. In an effort to battle breakthrough infections from Omicron, vaccine developers and manufacturers began reformulating their products, ushering bivalent boosters into use that utilize antigens from ancestral as well as Omicron variants of the spike protein (some companies switching entirely to omicron antigens)[16,17]. At the onset of the pandemic, the world's central focus was on the development of a safe and effective vaccine. The second stage of this effort was distribution, ensuring that as many people as possible were vaccinated to establish community immunity. Thanks to these efforts and a reduction in mortality due to preexisting immunity, SARS-CoV-2 has begun taking on the characteristics of an endemic pathogen, likely to require a continued public health response effort [18–20].

Influenza is another endemic respiratory pathogen with comparable characteristics to SARS-CoV-2 [21]. The influenza virus can easily mutate and reassort its genome into novel strains capable of causing pandemics, oftentimes utilizing animal reservoirs as hosts for antigenic shift. This has been observed numerous times in history, with four prominent examples being the 1918 H1N1 Spanish flu pandemic, the 1957 H2N2 pandemic beginning in East Asia which due to antigen shift led the 1968 H3N2 pandemic and, more recently, the 2009 H1N1"swine flu" pandemic [22,23]. Each year, existing influenza strains in the population undergo antigenic drift and emerge in endemic "flu seasons," evading community immunity and previously acquired immunity from vaccines [24]. It is now expected that the major burden of COVID-19 in years to come will align with the seasonality of influenza cases, contributing to a compounded public health burden [25]. Considering the likely need to annually reformulate the COVID-19 vaccines to match emerging variants, it is essential to explore strategies for the rapid modification but also production of COVID-19 boosters. One such approach is employment of a vaccine platform for SARS-CoV-2 that can be mass produced using existing vaccine infrastructure- supporting the additional goals of reducing production costs and improving vaccine distribution, thus optimizing healthcare resources and reducing the overall burden of COVID-19 on the world's healthcare system.

Viruses make an attractive vaccine platform for eliciting systemic but also mucosal immunity that can protect against respiratory pathogens. Live attenuated influenza vaccines have been licensed for human use since 2003 and their efficacy when delivered via the intranasal route has been demonstrated by the use of FLUMIST [26,27]. Influenza viruses are easily modifiable and can be engineered to express non-influenza antigens in infected cells, inducing strong immune responses against these antigens [28–31]. Several modified influenza viruses have been developed and investigated for use as a vaccine platform against SARS-CoV-2 [32–34]. One of them, the candidate vaccine dNS1-RBD, progressed to clinical trials and usage in China [35,36]. dNS1-RBD was genetically engineered using the H1N1 influenza virus California/4/2009 (CA04-dNS1) as the vector's viral backbone and replacing the NS1 nonstructural nuclear export protein with the genetic sequence for SARS-CoV-2 RBD. The choice of viral backbone was made based on the suppressed replication of dNS1 at temperatures similar to that of the human lower respiratory tract—making it less likely to cause undesirable side effects related to the viral vector. Delivered intranasally, dNS1-RBD conferred protection against challenge with the SARS-CoV-2 Beta variant in the preclinical Syrian hamster model [36]. Human clinical trial data confirmed the safety of dSN1-RBD administered in a multi-dose format and found a low incidence rate of adverse effects. At its completion, trial data ultimately showed that dSN1-RBD was protective against infection with viruses from the omicron lineage [37]. Loes et al. reported on the development of another modified influenza virus expressing SARS-CoV-2 RBD which, when delivered to mice by the intranasal route, infected cells and generated high levels of anti-RBD IgG neutralizing antibodies [38]. ΔNA(RBD) flu (henceforth referred to as ΔNA(RBD) utilizes the A/WSN/33 influenza virus as its backbone but replaces the native hemagglutinin (HA) gene sequence with that of the A/Aichi/2/1968 H3 virus which features an attenuating amino acid mutation in the receptor binding site (Y98F) as well as an additional mutation (R453G) which was found to improve production titers of the ΔNA(RBD) virus. In place of the neuraminidase (NA) coding sequence, a SARS-CoV-2 RBD antigen sequence fused to a mouse CD80 C terminal region (B7.1) is inserted. This fusion allows for infected host cells to display membrane membrane-anchored SARS-CoV-2 RBD, which can then be subsequently processed by host immune cells.

In this study, we expanded the preclinical evaluation of ΔNA(RBD) as an intranasal COVID-19 vaccine and designed experiments to measure its protective capacity against SARS-CoV-2 viral challenge. Intranasal vaccination has been shown to induce localized mucosal immune responses and provide protection from COVID-19 and other respiratory infections [39–42]. K18-hACE2-mice were intranasally immunized with ΔNA(RBD) expressing SARS-CoV-2 ancestral or Omicron BA.1 variant RBD, then challenged with the Delta or Omicron strains of SARS-CoV-2. We observed robust RBD-specific IgG responses that correlated with protection against disease pathology and viral replication in the tissues. Overall, our data suggest the ΔNA(RBD) platform is an effective strategy to generate mucosal and systemic immunity. We expect this work will mark a valuable step forward in the development of intranasal vaccines for COVID-19 that utilize unique platforms.

Results

Mice vaccinated with Δ(NA)RBD flu virus generate strong anti-RBD responses

Influenza A viruses have been well studied and are known to be easily modifiable [27,30,34]. Additionally, they induce strong host immune responses upon infection characterized by high systemic IgG levels and the production of mucosal IgA antibodies [38,43]. This makes attenuated influenza viruses, which can be engineered to express additional antigens such as the SARS-CoV-2 RBD, highly valuable as vectors for vaccine development. In these studies we utilized the novel attenuated influenza virus ΔNA(RBD) (Fig. 1A-B) [38]. Δ(NA)RBD is constructed so that the coding sequence for RBD replaces the sequence for the influenza virus's neuraminidase (NA) protein. The engineered RBD sequence features a sequence encoding the murine immunoglobulin H chain V-region leader sequence on its N-terminus and encodes the transmembrane region and cytoplasmic domain of murine B7.1 on the sequence's C-terminus to ensure membrane tethering of RBD to the cell membrane upon expression. This entire RBD sequence is flanked with the native packaging signals of the viral NA coding region to ensure the full incorporation of RBD into the virion (Fig. 1A-B) [38]. Infection with Δ(NA)RBD causes surface expression of RBD on host cells, presenting the antigen in such a way that it can be processed by host antigen presenting cells and the immune system. When administered to mice intranasally, Δ(NA)RBD has been shown to induces high titers of anti-SARS-CoV-2 RBD IgG antibodies, with strong neutralizing function [38]. These results suggest that this platform could be effectively used as a vaccine.

To determine the efficacy of Δ(NA)RBD as a protective SARS-CoV-2

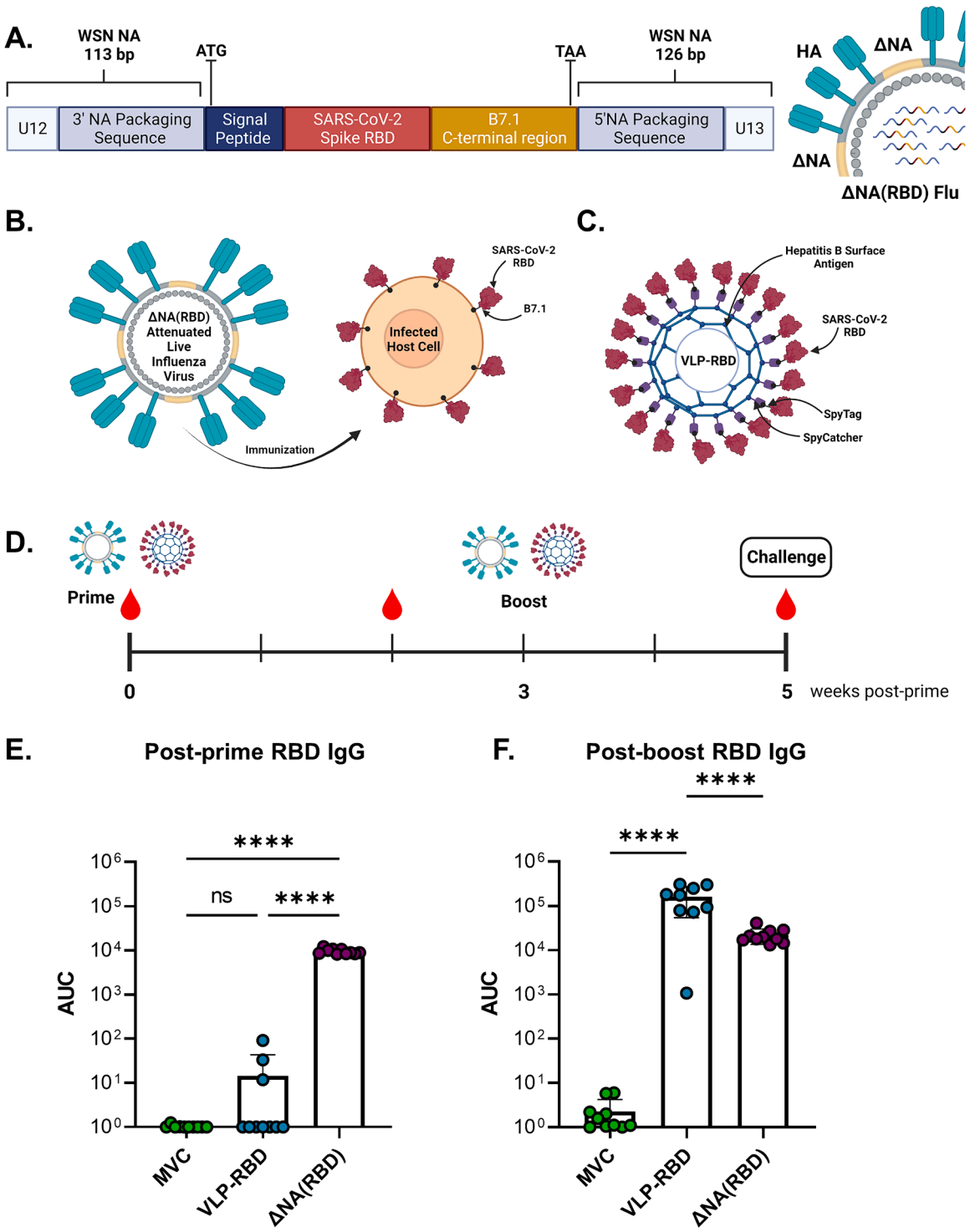

Fig. 1. ΔNA(RBD) Structure, mouse vaccination schedule, and antibody response data. (A) Diagram of the ΔNA(RBD) genome and illustration of virion featuring surface Hemagglutinin (HA), coding for RBD+B7.1 in the neuraminidase (NA) region. (B) Illustration of ΔNA(RBD) virus infecting a host cell and subsequent expression of membrane bound RBD by host cell. (C) Illustration of VLP-RBD construct, showing hepatitis B surface antigen joined with SAR-CoV-2 RBD via spy catcher/spy tag interaction [44,46]. (D) Timeline for K18-hACE2 mouse vaccination, serum collection, and challenge. n = 10 mice per group. (E) Anti-Ancestral RBD IgG titers of K18-hACE2 mouse serum collected 2 weeks post receipt of priming vaccine dose. (F) Anti-ancestral RBD IgG levels in K18-hACE2 mouse serum collected 2 weeks post vaccine boost dose. IgG titers are represented as log AUC. Results are represented as mean ± SD. Points represent individual mice, n = 10 mice per group. One-way ANOVA with Tukey's multiple comparison test was performed for statistical analysis: **** = $P < 0.0001$. MVC = Mock Vaccinated and Challenged.

vaccine, we designed preclinical experiments to compare intranasal Δ(NA)RBD vaccine to an intranasal RBD-expressing virus like particle (VLP) vaccine previously characterized by our lab (VLP-RBD) (Fig. 1C) [44]. We previously demonstrated that VLP-RBD confers protection against Delta and Omicron SARS-CoV-2 challenge in K18-hACE2 mice [44]. VLP-RBD utilizes the SpyTag/SpyCatcher system to irreversibly conjugate RBD proteins to the surface of a hepatitis B surface antigen, creating an antigen-rich virus like particle [45,46] (Fig. 1C). Despite a high antigen load, the VLP-RBD vaccine uses the adjuvant BECC470 to increase its immunogenicity and confer protection [47,48]. We

hypothesized that Δ(NA)RBD administered without an adjuvant would be highly immunogenic due to the capacity of an engineered live virus for infection and replication. To compare the humoral immune responses to both vaccines, K18-hACE2 mice were vaccinated with Phosphate Buffered Saline (PBS-control), VLP-RBD, or Δ(NA)RBD expressing ancestral SARS-CoV-2 RBD via the intranasal route. Three weeks after prime immunization, mice were administered a second boost dose (Fig. 1D). We found that mice vaccinated with Δ(NA)RBD developed levels of anti-RBD IgG antibodies in serum 2 weeks post prime vaccination which were significantly higher than those of VLP-RBD vaccinated mice (Mann-Whitney test $P < 0.0001$) (Fig. 1E). Boosting with a second dose significantly increased anti-RBD IgG antibody levels in both VLP-RBD vaccinated mice (Mann-Whitney test $P < 0.0001$) as well as in Δ(NA)RBD vaccinated mice (Mann-Whitney test $P < 0.0001$), however the fold increase in the VLP-RBD group was much larger than that of the Δ(NA)RBD group (greater than 11,000-fold vs 2-fold) (Fig. 1F). These data demonstrate the ability of Δ(NA)RBD to elicit a strong humoral immune response from the first dose of vaccine administered by the intranasal route. With a second dose, following the vaccine schedule of current COVID-19 vaccines, antibody levels increase, prompting studies to define the relationship between these antibody levels and protection.

Vaccination with Δ(NA)RBD limits disease pathology and morbidity following SARS-CoV-2 Delta challenge

Infection with the Delta variant of SARS-CoV-2 causes severe disease and morbidity in K18-hACE2 mice as demonstrated by our lab and others [49–52], making its infection pathology in K18-hACE2 mice a valuable preclinical model for assessing the capacity of novel COVID-19 vaccines to confer protection through reduced morbidity. We challenged PBS, Δ(NA)RBD, and VLP-RBD vaccinated K18-hACE2 mice 2 weeks after completion of our two-dose vaccine schedule with a 10^4 plaque forming units (PFU) intranasal dose of the Delta variant and monitored them over 10 days to track the development of disease pathology

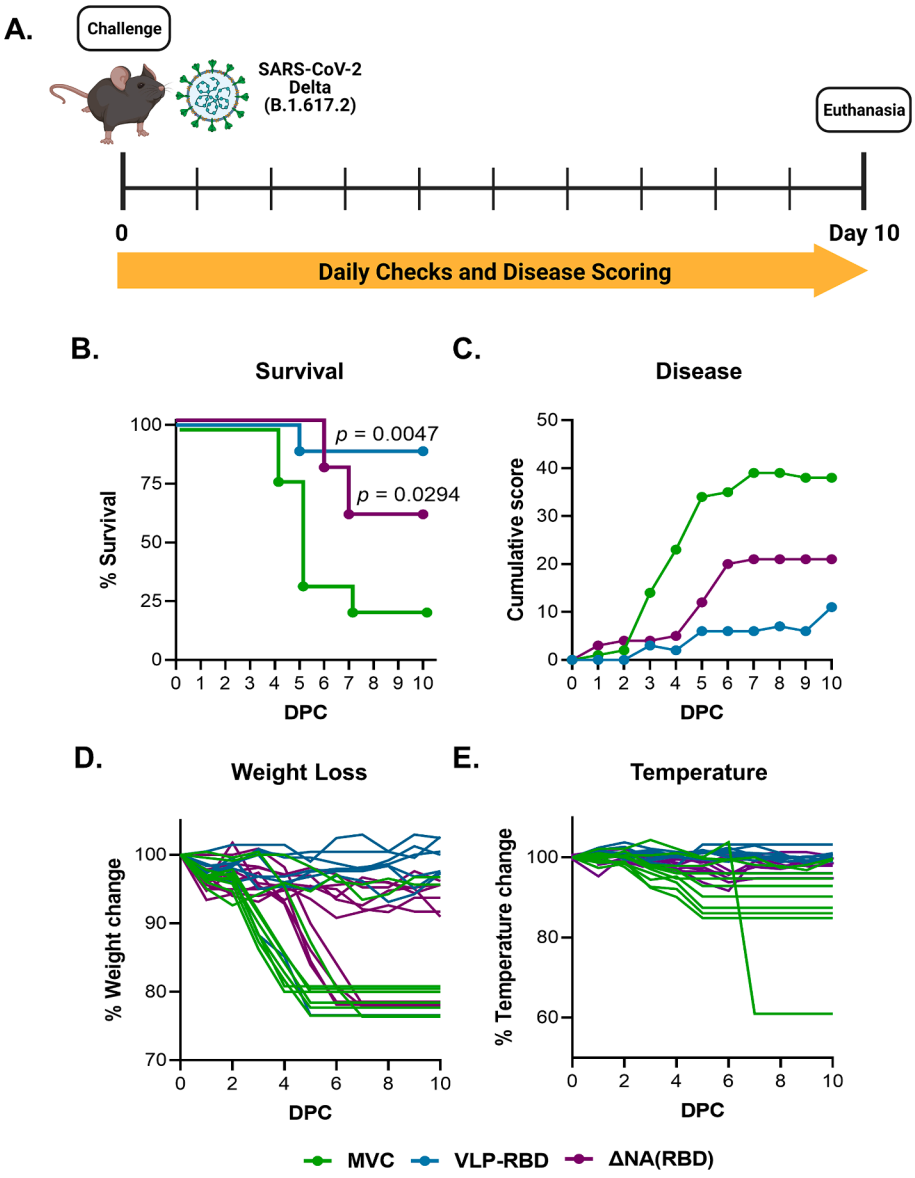

Fig. 2. Delta challenge study timeline and evaluation of humoral responses to vaccination. (A) Timeline for K18-hACE2 mouse challenge studies utilizing the SARS-CoV-2 Delta variant. (B) Kaplan Meier survival curves of K18-hACE2 mice post-challenge. Log-rank (Mantel-Cox) tests were used to measure significance against MVC. (C) Graph of the combined group disease scores (n = 10) from challenged K18-hACE2 mice up to 10 days post challenge with SARS-CoV-2 delta variant. (D) Graph displaying daily weight loss data of K18-HACE2 up to 10 days post challenge with SARS-CoV-2 delta variant. Lines represent individual mice. (E) Graph displaying changes in K18-hACE2 mouse rectal temperature measured daily up to 10 days post challenge. Lines represent individual mice.

(Fig. 2A). Mock-vaccinated control (MVC) mice displayed a survival rate of 20 % by the end of the experiment (Fig. 2B). VLP-RBD vaccinated mice showed the highest survival rate of 80 % at the end of the 10-day challenge window, and vaccination with Δ(NA)RBD improved mouse survival rates to 60 %, demonstrating that mice, compared to MVC, were partially protected against morbidity (Fig. 2B). With improved survival rates, Δ(NA)RBD vaccinated mice also showed reduced disease burden in the form of lower cumulative disease scores, less weight loss and relatively stable temperatures compared to the mock-vaccinated challenge group, although disease phenotypes were not as mild as those seen in the VLP-RBD group (Fig. 2C-E). These results show that while Δ(NA)RBD vaccination does not attenuate correlates of morbidity in K18-hACE2 mice to the extent that VLP-RBD does, the flu-based platform significantly improves survival and disease scores compared to mock-vaccinated mice.

Viral burden following Delta challenge in the lung, brain, and respiratory tract is reduced in Δ(NA)RBD vaccinated mice

To determine the effect of Δ(NA)RBD vaccination on viral burden post-challenge, we collected the brains, lungs, and performed nasal lavage on each experimental group of mice at euthanasia. Mice vaccinated with Δ(NA)RBD and VLP-RBD when compared to mock-vaccinated and challenged (MVC) mice showed lower copy numbers of the SARS-CoV-2 nucleocapsid gene in tissue samples analyzed via qRT-PCR. VLP-RBD vaccinated mice that succumbed to infection earlier than 10 days post challenge (indicated by red data points) were determined to have high copy numbers of the viral gene in the brain and lung compared to mice that survived (Fig. 3A,B). Notably, Δ(NA)RBD significantly limited the infiltration of virus into the brains of vaccinated mice compared to MVC mice ($P = 0.0015$) (Fig. 3A). While not statistically significant, Δ(NA)RBD vaccinated mice also had lower levels of viral copies in the lung tissue compared to controls (Fig. 3B). In nasal wash, mice that succumbed to infection before day 10 had similar viral copy numbers to the MVC group, and mice that survived to day 10 showed low copies of the nucleocapsid gene, nearly at the assay's limit of detection (Fig. 3C). In conclusion, these data suggest that Δ(NA)RBD vaccination reduces the burden of viral copies in disease relevant tissues after SARS-CoV-2 Delta challenge.

IgA responses after Delta challenge are high in Δ(NA)RBD vaccinated mice

Intranasal vaccination, like infection with a respiratory pathogen, can induce immune responses in the mucosal tissues of the respiratory tract that protect against future pathogen exposure [53,54]. One measurable correlate of these responses is IgA antibody production [55–57]. Our lab has previously observed an increase in the level of anti-RBD IgA in intranasally vaccinated mice following challenge with SARS-CoV-2 [44,49]. In this study, we measured anti-RBD IgA levels in the lung supernatants and nasal wash fluid of vaccinated mice after challenge using ELISA. Mice vaccinated with Δ(NA)RBD and VLP-RBD had higher levels of IgA in their lungs following Delta challenge compared to mock vaccinated mice (Fig. 4A). Both were determined to be significantly greater than those observed in the MVC group ($P < 0.0089$). IgA titers measured in the nasal wash of mice at euthanasia were extremely

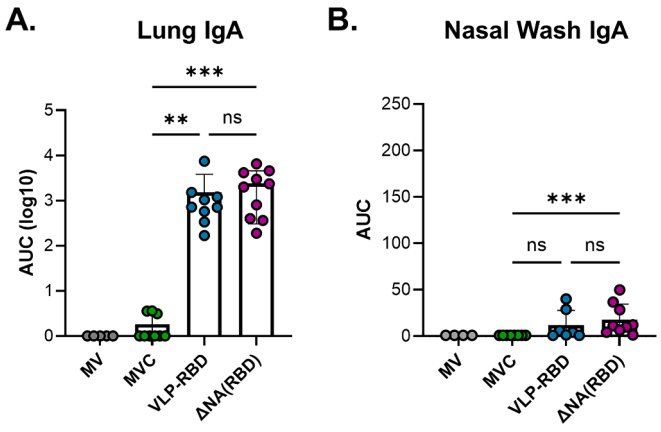

Fig. 4. RBD IgA antibody responses in vaccinated mice challenged with SARS-CoV-2 Delta variant. (A) Graph of anti-ancestral RBD IgA titers in the lungs of K18-hACE2 mice at euthanasia post-challenge quantitated via ELISA. (B) Graph of anti-RBD IgA titers in the Nasal Wash of K18-hACE2 mice measured via ELISA. IgA titers are represented as AUC. Results are represented as mean ± SD. Points represent individual mice, n = 10 mice per group. Points not passing outlier test were removed. Kruskal-Wallis tests with multiple comparisons were used for statistical analyses. *$P < 0.0112$, ** = $P < 0.0089$, *** = $P < 0.0007$.

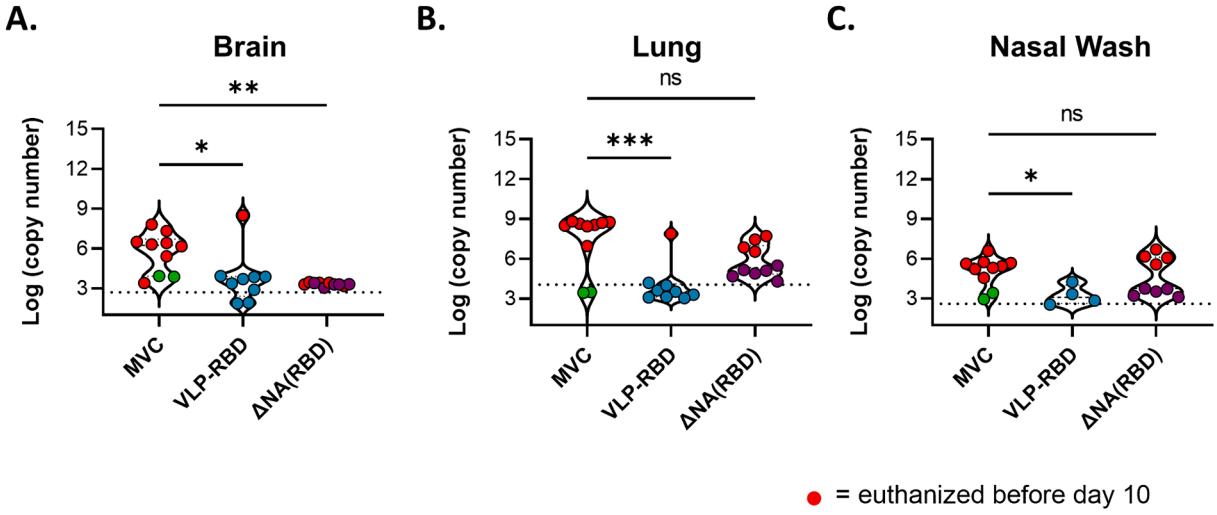

Fig. 3. qRT-PCR of SARS-CoV-2 nucleocapsid gene RNA in vaccinated mouse lungs post Delta challenge. (A) Violin plot depicting the SARS-CoV-2 viral nucleocapsid RNA copies in (A) brain homogenates, (B) lung homogenates, and (C) nasal wash fluid of challenged mice collected at euthanasia. Points represent individual mice, n = 10 mice per group. Dotted lines represent the median of each group. Dashed line indicates limit of detection calculated from analysis of tissues from no-vaccine no-challenge K18-hACE2 mice. One-way ANOVA with Tukey's multiple comparison test was performed for statistical analyses: * = $P < 0.05$, ** = $P < 0.01$, *** = $P < 0.001$.

low, however, a slight significant increase was detected in the levels of IgA in Δ(NA)RBD vaccinated mice compared to those in MVC ($P = 0.0007$) (Fig. 4B). In conclusion, mice vaccinated with Δ(NA)RBD had elevated levels of IgA in their lungs and nasal cavity compared to non-vaccinated control mice which suggests the development of mucosal immune responses that aided in protection against Delta challenge.

Immunization with an Omicron strain of Δ(NA)RBD improves antibody responses towards the Omicron SARS-CoV-2 variant

The most predominant strains of SARS-CoV-2 across the globe in 2023 come from the Omicron variant lineage [6]. These viruses are distinct from previous variants of SARS-CoV-2, featuring many mutations that impact transmissibility, allow the viruses to outcompete earlier strains in the population [8,9,58]. One worrisome facet of the rise to dominance of the Omicron variant is its ability to evade the immune system as well as prior protection afforded by convalescence or vaccination [20,58,59]. For this reason, we hypothesized that changing the RBD antigen expressed by Δ(NA)RBD from an ancestral RBD (Δ(NA)RBD) to Omicron RBD (Δ(NA)RBD Omicron) would be critical to ensuring protection in an Omicron challenge model. We generated a Δ(NA)RBD strain encoding RBD from the Omicron BA.1 virus with rpk9 stabilizing mutations [60], and vaccinated K18-hACE2 mice by the intranasal route, this time using a slightly higher dose in an effort to also improve the immune responses demonstrated previously. Controls of a matched dose of intranasal Δ(NA)RBD and an intramuscular 10 μg dose of a COVID-19 mRNA vaccine (previously used by our lab to confer protection in mice [44] were used for making comparisons. Mice were vaccinated following a four-week prime/boost schedule to follow that of human mRNA COVID-19 vaccines (Fig. 5A). K18-hACE2 mice

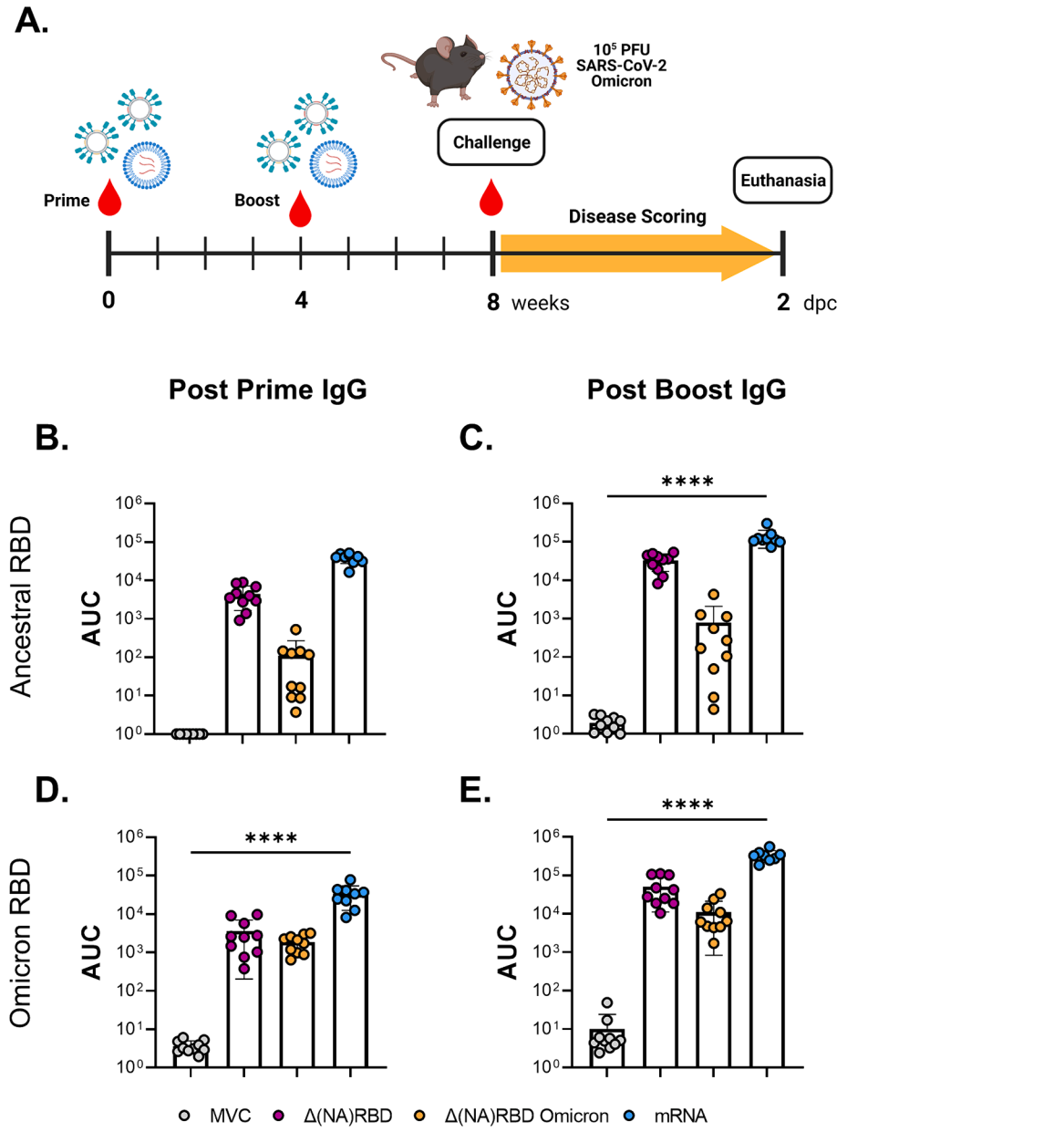

Fig. 5. Omicron challenge study timeline and humoral responses to vaccination. (A) Illustrated timeline of the vaccination and subsequent challenge of K18-hACE2 with SARS-CoV-2 Omicron BA.5 variant. (B-C) Graphs displaying anti-ancestral RBD IgG titers in serum collected two weeks post priming vaccine dose (B) and two weeks post booster vaccine dose (C). (D-E) Graphs displaying anti-Omicron RBD IgG titers in serum collected two weeks post priming vaccine dose (E), and two weeks post booster vaccine dose (F). IgG titers are represented as log AUC. Results are represented as mean ± SD. Points represent individual mice, n = 10 mice per group. One-way ANOVA with Tukey's multiple comparison test was performed for statistical analysis: **** = $P < 0.0001$.

vaccinated with the original Δ(NA)RBD virus were determined to have higher levels of IgG specific to the ancestral variant RBD than Δ(NA)RBD Omicron after priming and boosting (Fig. 5B, C). At both timepoints though, these antibody levels did not surpass those of mRNA-vaccinated mice. We repeated antibody analyses by ELISA using Omicron variant RBD (variant B.1.1.529). Interestingly, although there was no significant difference in IgG levels against Omicron RBD in serum from either Δ(NA)RBD strain after priming (Fig. 5D), Omicron RBD IgG levels after boost were again significantly higher in mice vaccinated with the ancestral virus than those in the omicron virus vaccinated mice (Fig. 5E).

Due to the replicating influenza virus backbone of Δ(NA)RBD, we considered that humoral responses would develop that are specific to the vector. Using serum collected at euthanasia, we used ELISA to measure anti-hemagglutinin (HA) IgG. In serum from mice vaccinated with mRNA vaccine we expectedly did not measure anti-HA IgG antibodies (Sup Fig. 1). Δ(NA)RBD and Δ(NA)RBD Omicron vaccinated mouse serum showed high levels of anti-HA IgG which were not statistically different between the two groups (Sup Fig. 1).

To assess the function of anti-RBD antibodies in conferring protection, we performed live virus neutralization assays. Cells were cultured with the Omicron BA.5 SARS-CoV-2 virus and dilutions of serum collected from vaccinated mice four weeks after boosting. After an incubation period, plates were then assessed for variations in plaque formation (Fig. 6A). Only serum from mRNA-vaccinated mice was able to limit Omicron BA.5 virus plaque formation *in vitro* at the lowest dilutions of 1:8 and 1:32 (Fig. 6B). Only two serum samples from mRNA vaccinated animals were able to limit plaque formation at the 1:128 dilution. One serum sample from each Δ(NA)RBD variant vaccinated group prevented plaque formation *in vitro* at the 1:8 dilution. At the 1:32 dilution, only one sample from Δ(NA)RBD Omicron vaccination showed some plaque reduction ability. At the highest dilutions, 1:128 to 1:2048 (data not shown), plaque numbers were uncountable across all experimental groups. Despite being determined to contain high titers of anti-RBD IgG antibodies, serum from mice vaccinated with either strain of Δ(NA)RBD was unable to reduce Omicron virus replication *in vitro*. It is possible that performing this assay using serum at a later timepoint would show different neutralization due to maturation of antibody responses. In summary, although Δ(NA)RBD with variant-matching can elicit high serum levels of anti-RBD IgG, it was not observed to generate neutralizing antibodies.

Δ(NA)RBD Omicron vaccination decreases viral burden following Omicron challenge in mice

While *in vitro* plaque reduction assays did not suggest that Δ(NA)RBD or Δ(NA)RBD Omicron vaccinated mice developed SARS-CoV-2 neutralizing antibodies in their serum, we aimed to assess if other correlates of protection were conferred using the K18-hACE2 mouse preclinical challenge model. Our lab previously developed and utilized the Omicron challenge model to evaluate the VLP-RBD platform [44]. Due to our lab and others observing reduced morbidity from Omicron challenge strains in K18-hACE2 mice [20,61], all mice were euthanized 2 days post challenge to evaluate levels of replicating virus in the lungs. mRNA or Δ(NA)RBD vaccinated K18-hACE2 mice were challenged with a 10^5 PFU dose of Omicron (BA.5) virus administered to the nares 4 weeks post boost vaccination (Fig. 5A). Plaque assay analysis of lung tissue at euthanasia showed that mice vaccinated with Δ(NA)RBD Omicron had a significant reduction ($P = 0.0010$) in replicating live virus compared to MVC mice (Fig. 7A). Viral burden was also significantly limited in mice vaccinated with the original strain of Δ(NA)RBD ($P = 0.0020$). No significant difference in lung PFUs was measured between groups of mice vaccinated with Δ(NA)RBD strains and mRNA. These results were echoed by qRT-PCR analysis of SARS-CoV-2 nucleocapsid gene copies in lung homogenate RNA collected at euthanasia. Mice vaccinated with either strain of Δ(NA)RBD had lower copies of viral genes in the lung (Fig. 7B). Despite an observable trend in higher viral copies in some Δ(NA)RBD vaccinated mice compared to the Δ(NA)RBD Omicron group, we did not calculate this difference to be statistically significant. These findings show that intranasal vaccination with Δ(NA)RBD expressing ancestral or Omicron RBD protect against SARS-CoV-2 activity in the lung. Vaccine antigen matching with Omicron RBD to the challenge strain, however, may strengthen this protection.

Vaccinated mice after Omicron challenge show low IgA responses in the lung and respiratory tract

Previous intranasal vaccines evaluated by our lab have demonstrated that vaccination prior to challenge increases IgA production in the respiratory tract after challenge.[44,62] Although Δ(NA)RBD vaccinated mice show high serum IgG production and are partially protected against SARS-CoV-2 Omicron challenge, our data suggests these serum antibodies do not neutralize. Because Δ(NA)RBD was administered by the intranasal route, and with the knowledge that IgA is an important correlate of protection for mucosal immunity, we sought to measure IgA production to in the lungs and nasal cavity of vaccinated mice after Omicron challenge to evaluate their possible role in protective

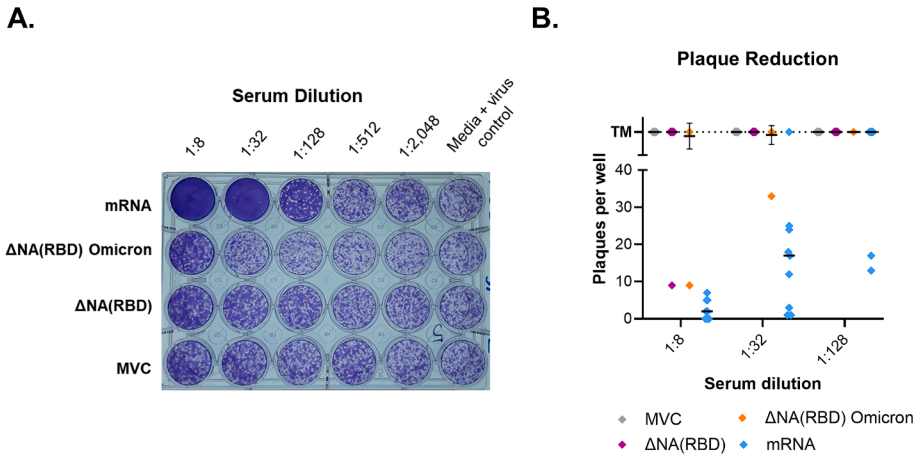

Fig. 6. *In vitro* plaque reduction assay using serum from vaccinated mice. (A) Image of an assay plate representing plaque reduction corresponding to serum dilutions in each treatment group. (B) Graph displaying results of *in vitro* plaque reduction assays using K18-hACE2 mouse serum collected 2-week post boost vaccination. Error bars represent mean + SEM. Wells designated "too many to count" were assigned arbitrary value for graphical purposes. TM = too many to count.

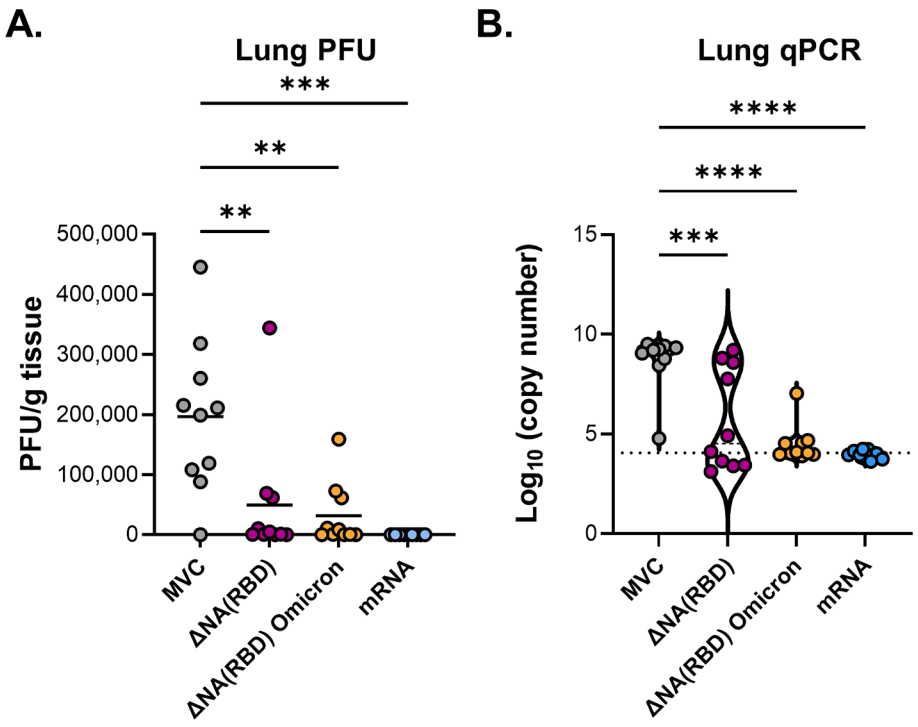

Fig. 7. PFU and SARS-CoV-2 nucleocapsid gene qRT-PCR data from the lungs of vaccinated K18-hACE2 mice post-Omicron variant challenge. (A) Graph displaying the PFU/gram of SARS-CoV-2 virus in lung tissue supernatants of vaccinated mice two days post-viral challenge. Bars indicate group mean. (B) Violin plot depicting the SARS-CoV-2 viral nucleocapsid RNA copies in lung tissue homogenates two days post-viral challenge. Dashed line indicates the assay's limit of detection calculated from analysis of lung tissue RNA from no-vaccine no-challenge K18-hACE2 mice. Points represent individual mice, n = 10 mice per group. One way ANOVA with Tukey's multiple comparisons test was used for statistical analysis: ** = $P < 0.0037$, *** = $P < 0.00071$, **** = $P < 0.0001$.

immunity. Interestingly, although Δ(NA)RBD vaccinated mice showed high levels of anti-RBD IgA after Delta SARS-CoV-2 challenge (Fig. 4), these antibodies were not detected in the lungs (Fig. 8A) or nasal wash (Fig. 8B) after Omicron challenge. Thinking that IgA antibodies may be generated specific to Omicron variant RBD we repeated the assay, coating with Omicron RBD and still did not detect anti-RBD IgA in the lung (Fig. 8C) or nasal wash (Fig. 8D). This data shows that IgA antibodies did not contribute to the protection against viral burden that was observed in the lungs of Δ(NA)RBD or Δ(NA)RBD Omicron vaccinated mice. Whether this data is the result of a euthanasia timepoint earlier than the start of IgA production, or possibly that of Omicron infection kinetics not inducing a strong mucosal antibody response remains to be determined.

Discussion

COVID-19 is transitioning from a pandemic disease to one that is likely to be endemic and predicted to reemerge seasonally [63]. Breakthrough transmission and infection of the SARS-CoV-2 virus from vaccinated hosts suggests that regular boost vaccination will be increasingly necessary for renewing immunity within the population. This phenomenon is also applicable to endemic influenza seasons, where the vaccines are reformulated yearly to protect vulnerable populations against current variants of the influenza virus. In this study we evaluated the protective efficacy of ΔNA(RBD), an easily modified viral vectored vaccine, against SARS-CoV-2 variant challenge in the K18-hACE2 preclinical mouse model of COVID-19. We demonstrated that immunization with ΔNA(RBD) elicits strong serum IgG antibody levels that correlate to protection against disease-characteristic morbidity after Delta variant challenge. ΔNA(RBD) vaccinated mice were 60% protected against morbidity after Delta variant challenge, and surviving mice showed low viral burden in the lungs, nasal wash, and importantly did not show viral dissemination into the brain while mock vaccinated mice did. Vaccinated mice also produced high titers of mucosal IgA after challenge in the respiratory tract which was similar to the highly protective intranasal VLP-RBD vaccine evaluated by our lab. Importantly, we showed that modification of ΔNA(RBD) to match vaccine antigen to challenge variant protected mice against the clinically relevant Omicron variant and lowered viral burden in the lungs. This study demonstrated that antigen matching to clinically relevant SARS-CoV-2 strains like Omicron can result in some loss of humoral immunity against ancestral-type strains. ΔNA(RBD) expressing Omicron RBD was found to induce strong Omicron specific antibody responses, but lower ancestral RBD IgG antibody responses. While these antibodies were not observed to exhibit neutralizing function *in vitro,* these antibodies correlated to lower levels of viral RNA detectable in the lungs of mice after Omicron challenge. Together, these data demonstrate that genetically modified influenza viruses could be useful as vectors for seasonably modifiable COVID-19 vaccines.

Intranasal vaccines are an attractive immunization approach known to induce strong mucosal immune responses, including IgA antibodies, that help to protect the respiratory tract from infection [64]. Traditional vaccination through intramuscular administration produces strong systemic IgG responses which can protect against severe disease, but can also fail to prevent breakthrough infections in the upper respiratory tract due to low tissue localization of IgG [65,66]. This can contribute to the incidence of breakthrough transmission in vaccinated hosts as well as asymptomatic infection rates. In our study, we observed that ΔNA(RBD) administered to mice by the intranasal route can induce high lung IgA responses to RBD antigen in immunized mice post Delta challenge. Antigen specific IgA antibodies in the lungs were comparable to our previously tested intranasal VLP-RBD vaccine, and titers in the nasal wash were found to be significantly higher (Fig. 4)[44]. IgG titers at 2 weeks post prime were also higher in ΔNA(RBD) vaccinated animals compared to those vaccinated with VLP-RBD suggesting that ΔNA(RBD), a live virus-based vector, perhaps develops systemic antibody responses

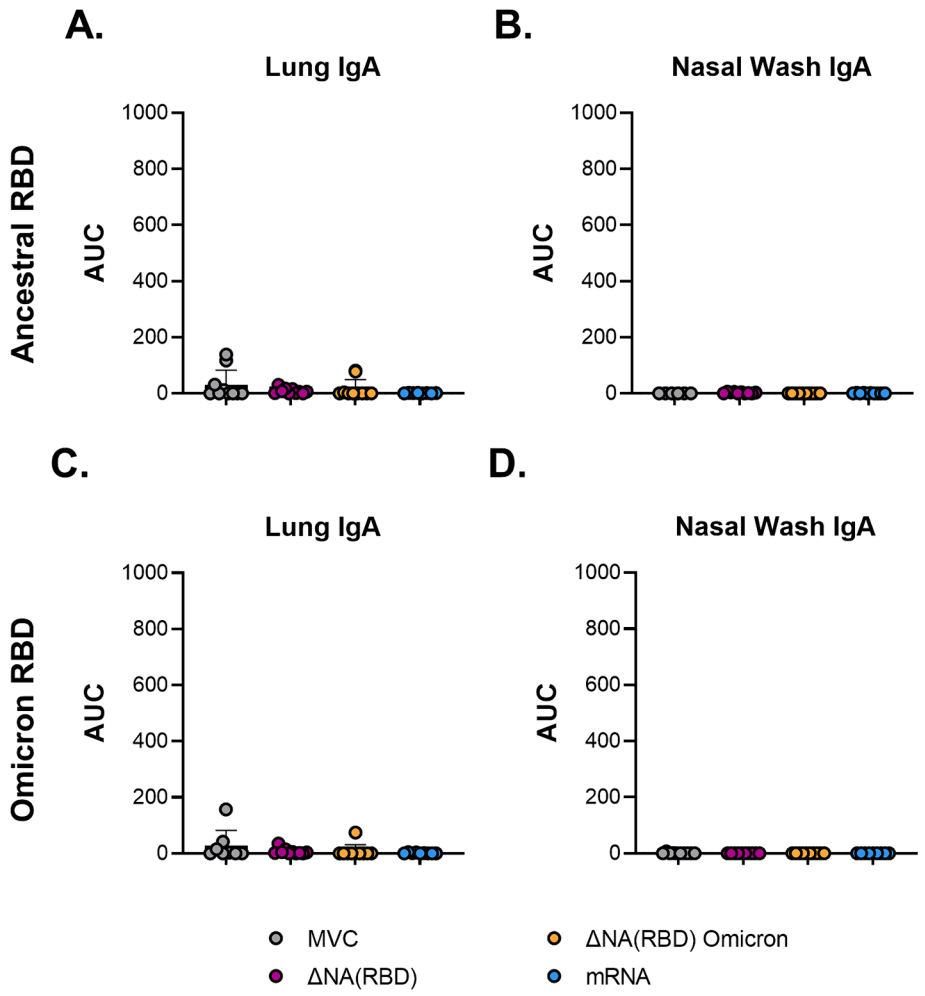

Fig. 8. Anti-ancestral or −Omicron RBD IgA levels in vaccinated mouse lungs and nasal wash two days post challenge. (A-B) Graphs of ELISA data quantitating anti-ancestral RBD IgA titers in the lungs (A) and nasal wash fluid (B) of vaccinated mice collected two days post-Omicron challenge. (C-D) Graphs of anti-Omicron RBD IgA titers in the lungs (C) and nasal wash (D) of vaccinated collected post challenge. IgA titers are presented as AUC. Results are represented as mean ± SD. Points represent individual mice, n = 10 mice per group.

more rapidly than a virus like particle (Fig. 1E). ΔNA(RBD) also generated higher mucosal IgA titers and similar serum IgG titers compared to our previously evaluated novel intranasal SARS-CoV-2 vaccine, BREC-CoV-2 [49]. However, this IgA response towards RBD was lost in Omicron challenge, which could be due to the experiment's early endpoint at day 2 not allowing time for IgA responses to expand. It is possible that IgA specific to RBD is produced later; however, this experiment prioritized evaluating viral burden as a correlate of protection rather than disease phenotypes as these are minimal in the murine Omicron challenge model. Many characteristics of ΔNA(RBD) induced immunity remain to be investigated in future studies such as the durability of this response, the cellular correlates of immunity, and its ability to prevent transmission or asymptomatic infections.

Currently, the only approved and utilized intranasal vaccine for human use is the influenza vaccine FLUMIST®, which is an attenuated live virus vaccine used to combat seasonal influenza via induction of localized mucosal immune responses [53,67]. Similarly, ΔNA(RBD) is a live attenuated virus, which likely allowed it to produce strong mucosal and systemic immune responses towards SARS-CoV-2. Modified adenovirus vector vaccines have also shown promising results in preclinical evaluations when administered intranasally, showing similar IgA responses to those demonstrated in this study, and have been shown to reduce SARS-CoV-2 transmission and offer protection in different animal models [68–72]. Both influenza and adenovirus vaccine platforms use an attenuated virus as a delivery system for an antigen of interest and generate systemic IgG responses through the replication and production of antigen in host cells. One important caveat to consider in the utilization of these types of vaccines is the limitation of immune responses by preexisting host memory. It has been demonstrated that prior exposure to adenoviruses, which commonly infect children to cause mild or asymptomatic disease, limits the development of adenovirus vectored vaccine immunity [73,74]. It is suggested that this issue can be circumvented by the use of adenovirus backbones that don't commonly infect humans or mutations to the highly variable regions of the commonly utilized human adenovirus serotype 5 virus (HAd5)[73]. The potential for pre-existing immunity from prior flu seasons towards the ΔNA(RBD) virus strain could also reduce its effectiveness in individuals with naturally acquired immunity. Pre-existing anti-HA responses generated from the priming dose of vaccine could also explain why the subsequent booster dose failed to further expand titers in this study. In summary, the immune responses and protection granted by ΔNA(RBD) vaccination are efficacious and show similar promise to the numerous intranasal vaccine platforms being developed, but the utilization of human viruses as vectors for vaccines carries important considerations [43,69,75,76].

In order to implement intranasal COVID-19 vaccines as disease-mitigating strategies, it will be necessary to understand the dynamics of intranasal boosting with pre-existing memory from intramuscular doses of mRNA or protein vaccines. It is estimated that more than 70 % of the global population has received at least one dose of a COVID-19

vaccine [77], which will inevitably begin to shape the systemic immune response to future infections and vaccinations. Intranasal ΔNA(RBD) vaccination produced strong systemic IgG responses towards RBD; however, these antigen specific antibodies were lower than those induced by intramuscular mRNA-1273 vaccination. Serum from mRNA vaccinated mice also exhibited higher virus neutralization in *in vitro* plaque reduction assays when compared to ΔNA(RBD)-vaccinated mice. While further investigation into defining the minimum protective dose of mRNA vaccine for the K18-hACE2 model will be valuable for ensuring appropriate comparisons, these studies showed the strength of the intramuscular mRNA platform in generating protective IgG dominated humoral responses. mRNA vaccination in the muscle does not generate the robust IgA responses seen in mice vaccinated with VLP-RBD or ΔNA (RBD), which we and other groups hypothesize are integral for mucosal immunity against respiratory pathogens. A valuable future area of study will be to investigate whether a dose of intranasally administered vaccine is capable of expanding the systemic memory responses of a previously administered intramuscular vaccine into the mucosa. Changing the location of the immune response may offer superior durable protection.

ΔNA(RBD) may represent an opportunity to utilize a combination vaccine for influenza and COVID-19. Administration of multiple vaccines at once, whether that be in separate formulations or as co-formulations, is extremely attractive for combatting poor vaccine uptake in the population. This approach is also commonly observed in vaccine schedules for children. While outside the scope of this study, it's possible that humoral responses against the flu virus backbone of this vector could afford some protection against influenza challenge. ΔNA (RBD) vaccinated mice had high anti-HA-IgG responses in serum. Subsequent animal challenge studies using influenza would need to be conducted to ensure ΔNA(RBD) provides protection against influenza infection, although a different animal model may need to be used as the majority of human influenza viruses are not infectious or pathogenic in common laboratory mouse strains [78]. It may also be possible to engineer the ΔNA(RBD) platform to express additional antigens from different pathogens. One possibility to explore, which would meet an urgent public health need, would be a combination FLU+COVID-19 + RSV vaccine.

In conclusion, we have performed preclinical evaluation of the ΔNA (RBD) vaccine as a candidate intranasal COVID-19 vaccine. We observed that ΔNA(RBD) induces both strong systemic IgG responses and can also elicit mucosal IgA responses in K18-hACE2 mice. ΔNA(RBD) vaccination also afforded K18-hACE2 mice protection from lethal challenge with SARS-CoV-2 Delta variant and reduced viral burden from non-lethal challenge with the Omicron variant. We found that modifying ΔNA (RBD) to express Omicron RBD rather than ancestral RBD improves variant-specific protection. Future long-term studies with K18-hACE2 mice will need to be conducted to determine the longevity of ΔNA (RBD) vaccine induced immunity as well as evaluate additional areas of the vaccine-induced immune responses such as T cell responses. Furthermore, testing the idea of priming and boosting with ΔNA(RBD) viruses expressing antigens representing a wider variety of RBD and HA epitopes would be valuable for maximizing the platform's potential. The reverse genetics technique used to generate ΔNA(RBD) can easily incorporate a variety of antigens [79–83], allowing it to be used for vaccines against other non-respiratory pathogens such as West Nile Virus, *Bacillus anthracis*, botulinum neurotoxin, and HIV which have already been studied with attenuated influenza virus vaccines [28–31]. Overall, ΔNA(RBD) is an easily modifiable vaccine platform which can be used by the intranasal route to induce potent immune responses. ΔNA (RBD) can in principle be produced using existing influenza vaccine manufacturing capabilities and infrastructure, making it a valuable vaccine platform to continue exploring the utility of.

Materials and methods

Ethics and biosafety statement

Vaccination and challenge studies utilized female B6.Cg-Tg(K18-ACE2)2Prlmn/J transgenic mice purchased from Jackson Laboratory. Animal studies were conducted under West Virginia University IACUC protocol #2009036460. During the vaccination period, mice were housed in biosafety level 2 conditions. SARS-CoV-2 challenge studies were conducted in West Virginia University's biosafety level 3 laboratory under IBC protocol #20-09-03. After vaccination and challenge, mice were monitored for adverse reactions and symptoms of morbidity. Mice were humanely euthanized in accordance with our lab's disease scoring system (see below). Downstream analyses were performed in BSL2 laboratory spaces, after samples were treated with 1 % Triton X-100 (ThermoFisher Scientific) by volume or stored in TRIzol Reagent (Zymo R2050-1) to inactivate virus.

ΔNA(RBD)-Flu vaccination

ΔNA(RBD)-Flu expressing SARS-CoV-2 Wuhan or Omicron RBD was generated as described previously [38] and provided for challenge studies by the Bloom lab at Fred Hutchinson Cancer Center. Female 6 or 8-week-old K18-hACE2 mice were vaccinated by the intranasal route with 50 μL ΔNA(RBD)-Flu at a concentration of $2x10^5$ TCID50 (Wuhan RBD strain in study 1) or $1x10^6$ TCID50 (Wuhan RBD and Omicron RBD strains in study 2) under anesthesia with ketamine/xylazine (Patterson Veterinary 07–803-6637/Patterson Veterinary 07–808-1947). In the VLP-RBD-BECC vs ΔNA(RBD)-Flu comparison study, an identical boost dose of vaccine was administered 3 weeks after priming. In comparison studies of ΔNA(RBD)-Flu with mRNA-1273, mice were boosted 4 weeks after priming to match the human COVID-19 vaccine schedule.

Vaccine formulations and vaccination

VLP-RBD-BECC was prepared as described previously [44]. Briefly, 25 μg BECC470 (obtained from the Ernst lab at University of Maryland Baltimore) was sonicated in water before 10 μg RBD-HBsAg VLP was added and incubated for 2 h. At the time of vaccination, 10X PBS was added to bring the total dose volume to 50 μL then administered via the intranasal route to 6-week-old female K18-hACE2 mice under anesthesia with intraperitoneal (IP) injection of 80 mg/kg ketamine/xylazine (Patterson Veterinary 07-803-6637/Patterson Veterinary 07-808-1947). Three weeks after priming, mice were administered a second identical dose. mRNA-1273 (Moderna) was obtained from the pharmacy at WVU Medicine. Female 8-week-old K18-hACE2 mice were administered 50 μL (10 μg) mRNA in the hind flank at priming and boosted 4 weeks later with an identical dose.

SARS-CoV-2 challenge procedure of K18-hACE2 mice

SARS-CoV-2 Delta variant B.1.617.2 hCoV-19/USA/WV-WVU-WV118685/2021(GISAID Accession ID: EPI_ISL_1742834) stocks used previously [84,85] were isolated from a patient sample at West Virginia University that was then propagated in Vero E6 cells (ATCC-CRL-1586). After propagation, viral stocks were sequenced to confirm integrity and lack of mutations. Omicron (BA.5) virus stocks were provided by the labs of Dr. Luis Martinez-Sobrido and Dr. Jordi Torrelles at the Texas Biomedical Research Institute. Before challenge, vaccinated and control (PBS-vaccinated) K18-hACE2 mice were anesthetized with an IP injection of ketamine/xylazine then inoculated intranasally with 50 μL of Delta virus (10^4 PFU) or Omicron virus (10^5 PFU).

Post-challenge disease scoring

After SARS-CoV-2 challenge, K18-hACE2 mice were evaluated

through daily in-person health checks and using the SwifTAG video monitoring system to monitor disease progression. Daily rectal temperature and weight were recorded in addition to changes in activity, appearance, the occurrence of eye closure/conjunctivitis, and changes in respiration. Scores were awarded to mice based on the severity of disease phenotypes following a scale that is previously described [84–87]: weight loss (0–4), appearance (0–2), activity (0–3), eye closure (0–2), and respiration (0–2). Scores in each category were combined into one overall numerical score that was recorded for each day. Mice that received either a daily score of 5 or achieved 20 % weight loss before day 10 post-challenge were euthanized with an intraperitoneal dose of pentobarbital (brand) in accordance with predetermined humane endpoint criteria.

Euthanasia and tissue collection

K18-hACE2 mice were euthanized 10 days post-challenge or earlier due to humane endpoint criteria via an intraperitoneal injection of pentobarbital (390 mg/kg) (Patterson Veterinary 07–805-9296) followed by cardiac puncture. Cardiac puncture blood was centrifuged (13000 rpm for 5 min) to extract serum for serological analyses. Postmortem, lung and brain tissue were collected for histopathology, antibody analyses, and assessment of viral burden. Lung and brain tissues were homogenized in 1 mL 1X PBS using the gentleMACS dissociator (miltenyi). A portion of lung homogenate was centrifuged to collect tissue supernatant for antibody analyses. To measure antibodies and viral burden in the upper respiratory tract, 1 mL 1X PBS was pushed through the nasal pharynx by catheter and collected. Lung and brain homogenates as well as nasal wash were treated with TRIzol reagent) at a ratio of 1:1 for nasal wash samples and 1:3 for lung and brain homogenate.

SARS-CoV-2 RBD and influenza HA IgG ELISA

IgG antibodies produced by K18-hACE2 mice in response to vaccination and SARS-CoV-2 challenge were quantitated in serum using a previously described method [45,85,87]. High bind 96-well plates (Pierce 15041) were coated with 2 ng/μL SARS-CoV-2 RBD (GenScript) or influenza A H3N2 (A/Aichi/2/1968) Hemagglutinin Protein (Sino biologicals) in 1X PBS. Plates were incubated for 5 min on a plate shaker at 440 rpm at room temperature before being stored at 4 °C overnight. The next day plates were washed 3 times with a solution of 1X PBS+0.1 % tween 20 detergent (PBS Tween). Samples were diluted 1:20 in 1 % milk in PBS Tween and added to the top row of every other plate, then serially diluted 1:2 down the wells of 2 plates, leaving the final row of wells as a blank. Plates were then incubated on a plate shaker at 440 rpm for 1 h before washed 3 times with PBS Tween. Secondary antibody (goat anti-mouse IgG HRP; Novus Biologicals NB7539) diluted 1:2000 in 1 % milk in PBS Tween was added to all wells. Plates were incubated for another hour at 440 rpm before being washed 5 times with PBS Tween. TMB substrate was added to each well then plates were stored in the dark for 15 min to develop. Development was stopped using 2 N sulfuric acid, and absorbance was read at 450 nm on the Synergy H1 plate reader. Antibody levels in samples were quantified using area under the curve analysis in GraphPad Prism V9.4.1.

SARS-CoV-2 RBD IgA ELISA

IgA antibody levels in vaccinated mice post-challenge were measured in nasal wash and lung supernatant that was collected at euthanasia. The previously described protocol for IgG ELISAs was followed with the following adaptations: plates were coated with SARS-CoV-2 RBD (Wuhan or Omicron) and blocked, then nasal wash (undiluted) and lung supernatant (diluted 1:5 in 1 % milk in PBS tween) were diluted 1:2 down two plates. The samples were then incubated on a plate shaker at 440 rpm for 2 h at room temperature. Antibodies were detected using secondary goat anti-mouse IgA HRP (Novus Biologicals NB7504) diluted 1:1000 in 1 % nonfat milk-PBS-Tween20 added to all wells. Plates were developed as described above and absorbance was read at 450 nm on the Synergy H1 plate reader. Antibody levels in samples were quantified using area under the curve analysis in GraphPad Prism V9.4.1.

qPCR of SARS-CoV-2 viral copies

RNA from brain homogenate, lung homogenate, and nasal wash of virally challenged mice was purified using the Direct-zol RNA miniprep kit (Zymo Research R2053) according to the manufacturer's protocol. qPCR of the SARS-CoV-2 nucleocapsid gene was then performed each sample using the Applied Biosystems TaqMan RNA to CT One Step Kit (ThermoFisher Scientific 4392938) to measure the number of viral copies via transcript number with specifications for each reaction having been described previously [45,49,51].

SARS-CoV-2 plaque assay of lung tissue homogenate

Vero E6 ACE2/TMPRSS2 cells were plated at 150,000 cells per well in 12-well plates and incubated at 37 °C and 5 % CO2 for 24 h. Mouse lungs collected at euthanasia were weighed and then homogenized in 1 ml of PBS. Homogenate was then centrifuged at 15,000*g* for 5 min. Supernatant was collected from the homogenate and diluted first 1:3, 1:10, and then four tenfold serial dilutions all in media. Cell media was aspirated from the plated cells. 200 μl of sample dilutions were added to each well in duplicate. Plates were incubated at 37 °C and 5 % CO2 for 1 h while gently rocking plates by hand every 15 min. After incubation, 2 ml of 0.6 % carboxyl methylcellulose overlay was added to each well. Plates were then incubated at 37 °C and 5 % CO2 for 4 days. On day 4, overlay was aspirated from all wells. Wells were then fixed with 10 % neutral buffered formalin and stained with 0.1 % crystal violet solution.

SARS-CoV-2 plaque reduction assay

SARS-CoV-2 plaque reduction neutralization assays were performed based on procedures previously described for standard plaque assays and plaque reduction tests [88–91]. Vero E6 hACE2/hTMPRSS2 cells were cultured in DMEM with high glucose and pyruvate (Gibco catalog number 11995-065) supplemented with 10 % non-heat inactivated FBS, 10 mM HEPES, Penicillin-Streptomycin at 100 units/mL Penicillin and 100 μg/mL Streptomycin, 1X GlutaMAX, 0.55 μg/mL Amphotericin B, and 10 μg/mL Puromycin dihydrochloride. Vero E6 hACE2/hTMPRSS2 cells were plated at 75,000 cells per well in 24-well plates in 0.5 mL supplemented DMEM per well. The plated cells were incubated for 24 h at 37 °C and 5 % CO_2. Mouse serum collected post-boost was diluted 1:4 in virus diluent media (Gibco catalog number 11995-065, supplemented with 2 % non-heat inactivated FBS, 10 mM HEPES, Penicillin-Streptomycin at 100 units/mL Penicillin and 100 μg/mL Streptomycin, 1X GlutaMAX, and 0.55 μg/mL Amphotericin B), then diluted by four-fold serial dilutions. Dilutions were performed in 96-well plates.

SARS-CoV-2 Omicron BA.5 virus stock (4.5×10^6 PFU/mL) was diluted 1:50 in virus diluent media. The diluted mouse serum was mixed with the diluted virus at a 1:1 ratio (75 μl serum + 75 μl virus) in 96-well plates and incubated at room temperature for 30 min. The final serum dilutions after mixing with virus were 1:8, 1:32, 1:128, 1:512, and 1:2,048. The final virus dilution was 1:100. Before applying serum and virus, media was aspirated from the Vero E6 hACE2/hTMPRSS2 cells. To each well, 100 μl of sample (serum + virus) was added. The plates were incubated at 37 °C and 5 % CO_2 for 1 h, rocking the plates by hand every 15 min.

A viscous overlay of 0.6 % carboxy methylcellulose (1:1 2X DMEM supplemented with 4 % non-heat inactivated FBS, 20 mM HEPES, Penicillin-Streptomycin at 200 units/mL Penicillin and 200 μg/mL Streptomycin, 2X GlutaMAX, 1.1 μg /mL Amphotericin B, and 0.6 %

sodium bicarbonate with 1.2 % carboxy methylcellulose) was added to each well then plates were incubated at 37 °C and 5 % CO_2 for 4 days (96 h). At the end of this incubation, media was aspirated from each well and replaced with 10 % neutral-buffered formalin before they were incubated at room temperature for 30 min. Plates were washed three times with water and stained with 0.1 % crystal violet solution for 15 min. Plates were washed three times with water and dried overnight prior to counting plaques.

To calculate the percent neutralization, individual plaques in each well were counted by eye using a light box. Wells with plaques that were "too many to count" were designated as such.

Statistical analyses

Data sets collected in these experiments were statistically analyzed using GraphPad Prism version 9. Vaccination and challenge studies were conducted using 10 mice per group. All data sets following a normal distribution were compared using ordinary one-way ANOVA with Tukey's multiple comparisons tests. Data determined to not follow a Gaussian distribution were compared using Kruskal-Wallis tests. Comparisons between two groups were made using a Student's *t*-test. Survival curves to compare the protection of each vaccine after SARS-CoV-2 Delta or Omicron challenged were created using the Kaplan-Meier estimate.

Funding

F.H.D. and the Vaccine Development Center (VDC) are supported by Research Challenge grant number HEPC.dsr.18.6 from the Division of Science and Research, West Virginia Higher Education Policy Commission.

Credit authorship contribution statement

Nathaniel A. Rader: Data curation, Formal analysis, Investigation, Writing – original draft, Writing – review & editing. **Katherine S. Lee:** Conceptualization, Data curation, Formal analysis, Investigation, Methodology, Writing – original draft, Writing – review & editing. **Andrea N. Loes:** Conceptualization, Investigation, Methodology, Writing – review & editing. **Olivia A. Miller-Stump:** Investigation. **Melissa Cooper:** Conceptualization, Investigation. **Ting Y. Wong:** Investigation, Methodology. **Dylan T. Boehm:** Formal analysis, Investigation, Writing – review & editing. **Mariette Barbier:** Supervision, Writing – review & editing. **Justin R. Bevere:** Supervision. **F. Heath Damron:** Conceptualization, Supervision, Formal analysis, Investigation, Writing – review & editing.

Declaration of competing interest

The authors declare that they have no known competing financial interests or personal relationships that could have appeared to influence the work reported in this paper.

Data availability

Data will be made available on request.

Acknowledgements

We thank both Dr. Laura Gibson and Dr. Clay Marsh at the WVU Health Sciences center for their continued support to pre-clinical COVID-19 research. We'd like to thank the Jesse Bloom lab at Fred Hutchinson Cancer Center for both providing and allowing us to work with the ΔNA(RBD) virus. We'd also like to thank Drs. Matthew D.J. Dicks and Sumi Biswas (SpyBiotech) as well as Dr. Christopher Love (MIT) for the use of their VLP-RBD spytag platform. Thank you to Dr. Robert Ernst for the use of the BECC adjuvant. Thank you to Dr. Ivan Martinez, Michael Winters, and Travis Rawson for their propagation of the original SARS-CoV-2 Delta virus, and Dr. Luis Martinez-Sobrido and Dr. Jordi Torreles for supplying the Omicron BA.5 virus used in the pre-clinical challenge studies.

Appendix A. Supplementary material

Supplementary data to this article can be found online at https://doi.org/10.1016/j.jvacx.2024.100543.

References

[1] Li X, Wang W, Zhao X, Zai J, Zhao Q, Li Y, et al. Transmission dynamics and evolutionary history of 2019-nCoV. J Med Virol 2020;92:501. https://doi.org/10.1002/JMV.25701.
[2] Wu F, Zhao S, Yu B, Chen YM, Wang W, Song ZG, et al. A new coronavirus associated with human respiratory disease in China. Nature 2020;579:265. https://doi.org/10.1038/S41586-020-2008-3.
[3] Farhud DD, Mojahed N. SARS-COV-2 notable mutations and variants: a review article. Iran J Public Health 2022;51:1494. https://doi.org/10.18502/IJPH.V51I7.10083.
[4] Tang JW, Toovey OTR, Harvey KN, Hui DDS. Introduction of the South African SARS-CoV-2 variant 501Y.V2 into the UK. J Infect 2021;82:e8.
[5] Yang WT, Huang WH, Liao TL, Hsiao TH, Chuang HN, Liu PY. SARS-CoV-2 E484K mutation narrative review: epidemiology, immune escape, clinical implications, and future considerations. Infect Drug Resist 2022;15:373. https://doi.org/10.2147/IDR.S344099.
[6] CDC COVID Data Tracker: Variant Proportions n.d. https://covid.cdc.gov/covid-data-tracker/#variant-proportions (accessed June 22, 2023).
[7] Cao Y, Wang J, Jian F, Xiao T, Song W, Yisimayi A, et al. Omicron escapes the majority of existing SARS-CoV-2 neutralizing antibodies. Nature 2022;602:657. https://doi.org/10.1038/S41586-021-04385-3.
[8] Qu P, Evans JP, Faraone JN, Zheng YM, Carlin C, Anghelina M, et al. Enhanced neutralization resistance of SARS-CoV-2 Omicron subvariants BQ.1, BQ.1.1, BA.4.6, BF.7, and BA.2.75.2. Cell Host Microbe 2023;31:9. https://doi.org/10.1016/J.CHOM.2022.11.012.
[9] Tian D, Sun Y, Xu H, Ye Q. The emergence and epidemic characteristics of the highly mutated SARS-CoV-2 Omicron variant. J Med Virol 2022;94:2376–83. https://doi.org/10.1002/jmv.27643.
[10] WHO – COVID19 Vaccine Tracker n.d. https://covid19.trackvaccines.org/agency/who/ (accessed June 12, 2023).
[11] Accorsi EK, Britton A, Fleming-Dutra KE, Smith ZR, Shang N, Derado G, et al. Association between 3 doses of mRNA COVID-19 vaccine and symptomatic infection caused by the SARS-CoV-2 omicron and delta variants. JAMA 2022;327:639–51. https://doi.org/10.1001/JAMA.2022.0470.
[12] Pulliam JRC, van Schalkwyk C, Govender N, von Gottberg A, Cohen C, Groome MJ, et al. Increased risk of SARS-CoV-2 reinfection associated with emergence of Omicron in South Africa. Science 2022:376. https://doi.org/10.1126/SCIENCE.ABN4947.
[13] Lipsitch M, Krammer F, Regev-Yochay G, Lustig Y, Balicer RD. SARS-CoV-2 breakthrough infections in vaccinated individuals: measurement, causes and impact. Nat Rev Immunol 2021;2021:1–9. https://doi.org/10.1038/s41577-021-00662-4.
[14] Christensen PA, Olsen RJ, Long SW, Snehal R, Davis JJ, Saavedra MO, et al. Early signals of significantly increased vaccine breakthrough, decreased hospitalization rates, and less severe disease in patients with COVID-19 caused by the Omicron variant of SARS-CoV-2 in Houston, Texas. MedRxiv 2022. https://doi.org/10.1101/2021.12.30.21268560.
[15] Cele S, Jackson L, Khoury DS, Khan K, Moyo-Gwete T, Tegally H, et al. Omicron extensively but incompletely escapes Pfizer BNT162b2 neutralization. Nature 2021;602:654–6.
[16] COVID-19 Vaccine, Bivalent | Moderna | For Vaccine Recipients n.d. https://eua.modernatx.com/recipients?tc=ps_8za5qcb&cc=4003&utm_source=google&utm_medium=search&utm_campaign=bnd+booster&gclsrc=aw.ds&&gclid=CjwKCAjwhJukBhBPEiwAniIcNc9jWPx7xDVUk83Vr-nkUqKROFj2ucfpawgOVk8dd4k23z2oHUqQ1RoCHc0QAvD_BwE (accessed June 12, 2023).
[17] Scheaffer SM, Lee D, Whitener B, Ying B, Wu K, Jani H, et al. Bivalent SARS-CoV-2 mRNA vaccines increase breadth of neutralization and protect against the BA.5 Omicron variant. BioRxiv 2022. https://doi.org/10.1101/2022.09.12.507614.
[18] Phillips N. The coronavirus is here to stay - here's what that means. Nature 2021;590:382–4. https://doi.org/10.1038/D41586-021-00396-2.
[19] Miller MB, Ooi EE, Rhoads DD, Kulldorff M, Anderson DE, Lee H, et al. As omicron takes hold and other new variants arise, COVID-19 testing remains the universally agreed tool to effect transition from pandemic to endemic state. Front Public Heal 2022;10:883066. https://doi.org/10.3389/FPUBH.2022.883066.
[20] Shuai H, Chan JFW, Hu B, Chai Y, Yuen TTT, Yin F, et al. Attenuated replication and pathogenicity of SARS-CoV-2 B.1.1.529 Omicron. Nat 2022 2022:1–7. doi:10.1038/s41586-022-04442-5.
[21] Coronavirus disease (COVID-19): Similarities and differences between COVID-19 and Influenza n.d. https://www.who.int/news-room/questions-and-answers/item/

coronavirus-disease-covid-19-similarities-and-differences-with-influenza (accessed June 22, 2023).
[22] Past Pandemics | Pandemic Influenza (Flu) | CDC n.d. https://www.cdc.gov/flu/pandemic-resources/basics/past-pandemics.html (accessed June 12, 2023).
[23] Al Hajjar S, McIntosh K. The first influenza pandemic of the 21st century. Ann Saudi Med 2010;30:1. https://doi.org/10.4103/0256-4947.59365.
[24] How Flu Viruses Can Change: "Drift" and "Shift" | CDC n.d. https://www.cdc.gov/flu/about/viruses/change.htm (accessed June 23, 2023).
[25] Influenza and COVID-19: Five tips for a safer winter n.d. https://www.who.int/westernpacific/news-room/feature-stories/item/influenza-and-covid-19–five-tips-for-a-safer-winter (accessed June 23, 2023).
[26] Using Live, Attenuated Influenza Vaccine for Prevention and Control of Influenza n.d. https://www.cdc.gov/mmwr/preview/mmwrhtml/rr5213a1.htm%5C (accessed June 12, 2023).
[27] Carter NJ, Curran MP. Live attenuated influenza vaccine (FluMist®; Fluenz^{TM}): A review of its use in the prevention of seasonal influenza in children and adults. Drugs 2011;71:1591–622. https://doi.org/10.2165/11206860-000000000-00000/FIGURES/TAB17.
[28] Li J, Diaz-Arévalo D, Chen Y, Zeng M. Intranasal vaccination with an engineered influenza virus expressing the receptor binding subdomain of botulinum neurotoxin provides protective immunity against botulism and influenza. Front Immunol 2015:6. https://doi.org/10.3389/FIMMU.2015.00170.
[29] Muster T, Ferko B, Klima A, Purtscher M, Trkola A, Schulz P, et al. Mucosal model of immunization against human immunodeficiency virus type 1 with a chimeric influenza virus. J Virol 1995;69:6678–86. https://doi.org/10.1128/JVI.69.11.6678-6686.1995.
[30] Li Z-N, Mueller SN, Ye L, Bu Z, Yang C, Ahmed R, et al. Chimeric influenza virus hemagglutinin proteins containing large domains of the Bacillus anthracis protective antigen: protein characterization, incorporation into infectious influenza viruses, and antigenicity. J Virol 2005;79:10003–12. https://doi.org/10.1128/JVI.79.15.10003-10012.2005.
[31] Martina BEE, van den Doel P, Koraka P, van Amerongen G, Spohn G, Haagmans BL, et al. A recombinant influenza A virus expressing domain III of West Nile virus induces protective immune responses against influenza and West Nile virus. PLoS One 2011:6. https://doi.org/10.1371/JOURNAL.PONE.0018995.
[32] Zhang L, Jiang Y, He J, Chen J, Qi R, Yuan L, et al. Intranasal influenza-vectored COVID-19 vaccine restrains the SARS-CoV-2 inflammatory response in hamsters. Nat Commun 2023 141 2023;14:1–18. doi: 10.1038/s41467-023-39560-9.
[33] Deng S, Liu Y, Tam RCY, Chen P, Zhang AJ, Mok BWY, et al. An intranasal influenza virus-vectored vaccine prevents SARS-CoV-2 replication in respiratory tissues of mice and hamsters. Nat Commun 2023:14. https://doi.org/10.1038/S41467-023-37697-1.
[34] Chaparian RR, Harding AT, Hamele CE, Riebe K, Karlsson A, Sempowski GD, et al. A virion-based combination vaccine protects against influenza and SARS-CoV-2 disease in mice. J Virol 2022:96. https://doi.org/10.1128/JVI.00689-22.
[35] Ma Y, Li J, Cao Y, Li W, Shi R, Jia B, et al. Acceptability for the influenza virus vector COVID-19 vaccine for intranasal spray: A cross-sectional survey in Beijing, China. Hum Vaccines Immunother 2023:19. https://doi.org/10.1080/21645515.2023.2235963.
[36] Chen J, Wang P, Yuan L, Zhang L, Zhang L, Zhao H, et al. A live attenuated virus-based intranasal COVID-19 vaccine provides rapid, prolonged, and broad protection against SARS-CoV-2. Sci Bull 2022;67:1372–87. https://doi.org/10.1016/j.scib.2022.05.018.
[37] Zhu F, Huang S, Liu X, Chen Q, Zhuang C, Zhao H, et al. Safety and efficacy of the intranasal spray SARS-CoV-2 vaccine dNS1-RBD: a multicentre, randomised, double-blind, placebo-controlled, phase 3 trial. Lancet Respir Med 2023;11:1075–88. https://doi.org/10.1016/S2213-2600(23)00349-1.
[38] Loes AN, Gentles LE, Greaney AJ, Crawford KHD, Bloom JD. Attenuated influenza virions expressing the SARS-CoV-2 receptor-binding domain induce neutralizing antibodies in mice. Viruses 2020:12. https://doi.org/10.3390/V12090987.
[39] Seo SH, Jang Y. Cold-adapted live attenuated SARS-Cov-2 vaccine completely protects human ACE2 transgenic mice from SARS-Cov-2 infection. Vaccines 2020;8:1–17. https://doi.org/10.3390/VACCINES8040584.
[40] Wu H-Y, Nguyen HH, Russell MW. Nasal Lymphoid Tissue (NALT) as a mucosal immune inductive site. Scand J Immunol 1997;46:506–13. https://doi.org/10.1046/j.1365-3083.1997.d01-159.x.
[41] Feng L, Wang Q, Shan C, Yang C, Feng Y, Wu J, et al. An adenovirus-vectored COVID-19 vaccine confers protection from SARS-COV-2 challenge in rhesus macaques. Nat Commun 2020:11. https://doi.org/10.1038/S41467-020-18077-5.
[42] Locht C, Papin JF, Lecher S, Debrie A-S, Thalen M, Solovay K, et al. Live attenuated pertussis vaccine BPZE1 protects baboons against bordetella pertussis disease and infection. J Infect Dis 2017;216:117–24. https://doi.org/10.1093/infdis/jix254.
[43] Liu X, Luongo C, Matsuoka Y, Park HS, Santos C, Yang L, et al. A single intranasal dose of a live-attenuated parainfluenza virus-vectored SARS-CoV-2 vaccine is protective in hamsters. Proc Natl Acad Sci USA 2021:118. https://doi.org/10.1073/PNAS.2109744118/-/DCSUPPLEMENTAL.
[44] Lee KS, Rader NA, Miller OA, Cooper M, Wong TY, Amin MS, et al. Intranasal VLP-RBD vaccine adjuvanted with BECC470 confers immunity against Delta SARS-CoV-2 challenge in K18-hACE2-mice. BioRxiv 2023. https://doi.org/10.1101/2023.04.25.538294.
[45] Wong TY, Russ BP, Lee KS, Miller OA, Kang J, Cooper M, et al. RBD-VLP Vaccines adjuvanted with alum or SWE protect K18-hACE2 Mice AGAINST SARS-CoV-2 VOC challenge. MSphere 2022:7. https://doi.org/10.1128/MSPHERE.00243-22/SUPPL_FILE/MSPHERE.00243-22-S0007.PDF.
[46] Rodriguez-Aponte SA, Dalvie NC, Wong TY, Johnston RS, Naranjo CA, Bajoria S, et al. Molecular engineering of a cryptic epitope in Spike RBD improves manufacturability and neutralizing breadth against SARS-CoV-2 variants. Vaccine 2023;41:1108. https://doi.org/10.1016/J.VACCINE.2022.12.062.
[47] Haupt RE, Harberts EM, Kitz RJ, Strohmeier S, Krammer F, Ernst RK, et al. Novel TLR4 adjuvant elicits protection against homologous and heterologous Influenza A infection. Vaccine 2021;39:5205–13. https://doi.org/10.1016/j.vaccine.2021.06.085.
[48] Gregg KA, Harberts E, Gardner FM, Pelletier MR, Cayatte C, Yu L, et al. A lipid A-based TLR4 mimetic effectively adjuvants a Yersinia pestis rF-V1 subunit vaccine in a murine challenge model. Vaccine 2018;36:4023. https://doi.org/10.1016/J.VACCINE.2018.05.101.
[49] Wong TY, Lee KS, Russ B, Horspool AM, Kang JK, Winters M, et al. Intranasal administration of BReC-CoV-2 COVID-19 vaccine protects K18-hACE2 mice against lethal SARS-CoV-2 challenge [Accepted Jan. 20, 2022 PMCID: PMC Journal - In Process]. Npj Vaccines 2022.
[50] Saito A, Irie T, Suzuki R, Maemura T, Nasser H, Uriu K, et al. Enhanced fusogenicity and pathogenicity of SARS-CoV-2 Delta P681R mutation. Nature 2021. https://doi.org/10.1038/S41586-021-04266-9.
[51] Lee KS, Wong TY, Russ BP, Horspool AM, Miller OA, Rader NA, et al. SARS-CoV-2 Delta variant induces enhanced pathology and inflammatory responses in K18-hACE2 mice. BioRxiv 2022. https://doi.org/10.1101/2022.01.18.476863.
[52] Liu X, Mostafavi H, Ng WH, Freitas JR, King NJC, Zaid A, et al. The Delta SARS-CoV-2 variant of concern induces distinct pathogenic patterns of respiratory disease in K18-hACE2 transgenic mice compared to the ancestral strain from Wuhan. MBio 2022. https://doi.org/10.1128/MBIO.00683-22.
[53] Barría MI, Garrido JL, Stein C, Scher E, Ge Y, Engel SM, et al. Localized mucosal response to intranasal live attenuated influenza vaccine in adults. J Infect Dis 2013;207:115. https://doi.org/10.1093/INFDIS/JIS641.
[54] Afkhami S, D'Agostino MR, Zhang A, Stacey HD, Marzok A, Kang A, et al. Respiratory mucosal delivery of next-generation COVID-19 vaccine provides robust protection against both ancestral and variant strains of SARS-CoV-2. Cell 2022;185:896–915.e19. https://doi.org/10.1016/J.CELL.2022.02.005.
[55] King RG, Silva-Sanchez A, Peel JN, Botta D, Dickson AM, Pinto AK, et al. Single-dose intranasal administration of AdCOVID elicits systemic and mucosal immunity against SARS-CoV-2 and fully protects mice from lethal challenge. Vaccines 2021:9. https://doi.org/10.3390/VACCINES9080881.
[56] Zhou R, Wang P, Wong YC, Xu H, Lau SY, Liu L, et al. Nasal prevention of SARS-CoV-2 infection by intranasal influenza-based boost vaccination in mouse models. EBioMedicine 2022;75:103762. https://doi.org/10.1016/j.ebiom.2021.103762.
[57] Takaki H, Ichimiya S, Matsumoto M, Seya T. Mucosal immune response in nasal-associated lymphoid tissue upon intranasal administration by adjuvants. J Innate Immun 2018;10:515–21. https://doi.org/10.1159/000489405.
[58] Yuan S, Ye ZW, Liang R, Tang K, Zhang AJ, Lu G, et al. Pathogenicity, transmissibility, and fitness of SARS-CoV-2 Omicron in Syrian hamsters. Science (80-) 2022;377:428–33. doi: 10.1126/science.abn8939.
[59] Saxena SK, Kumar S, Ansari S, Paweska JT, Maurya VK, Tripathi AK, et al. Characterization of the novel SARS-CoV-2 Omicron (B.1.1.529) variant of concern and its global perspective. J Med Virol 2022;94:1738–44. https://doi.org/10.1002/JMV.27524.
[60] Ellis D, Brunette N, Crawford KHD, Walls AC, Pham MN, Chen C, et al. Stabilization of the SARS-CoV-2 Spike receptor-binding domain using deep mutational scanning and structure-based design. Front Immunol 2021;12:710263. https://doi.org/10.3389/FIMMU.2021.710263/FULL.
[61] Halfmann PJ, Iida S, Iwatsuki-Horimoto K, Maemura T, Kiso M, Scheaffer SM, et al. SARS-CoV-2 Omicron virus causes attenuated disease in mice and hamsters. Nat 2022;2022:1. https://doi.org/10.1038/s41586-022-04441-6.
[62] Wong TY, Lee KS, Russ BP, Horspool AM, Kang J, Winters MT, et al. Intranasal administration of BReC-CoV-2 COVID-19 vaccine protects K18-hACE2 mice against lethal SARS-CoV-2 challenge. npj Vaccines 2022:7. https://doi.org/10.1038/S41541-022-00451-7.
[63] Contreras S, Iftekhar EN, Priesemann V. From emergency response to long-term management: the many faces of the endemic state of COVID-19. Lancet Reg Heal - Eur 2023;30:100664. https://doi.org/10.1016/j.lanepe.2023.100664.
[64] Chavda VP, Vora LK, Pandya AK, Patravale VB. Intranasal vaccines for SARS-CoV-2: From challenges to potential in COVID-19 management. Drug Discov Today 2021;26:2619–36. https://doi.org/10.1016/J.DRUDIS.2021.07.021.
[65] Bleier BS, Ramanathan M, Lane AP. COVID-19 vaccines may not prevent nasal SARS-CoV-2 infection and asymptomatic transmission. Otolaryngol Head Neck Surg 2021;164:305–7. https://doi.org/10.1177/0194599820982633.
[66] Kashte S, Gulbake A, El-Amin SF, Gupta A. COVID-19 vaccines: rapid development, implications, challenges and future prospects. Hum Cell 2021;34:711–33. https://doi.org/10.1007/S13577-021-00512-4.
[67] Gianchecchi E, Manenti A, Kistner O, Trombetta C, Manini I, Montomoli E. How to assess the effectiveness of nasal influenza vaccines? Role and measurement of sIgA in mucosal secretions. Influenza Other Respi Viruses 2019;13:429. https://doi.org/10.1111/IRV.12664.
[68] Van Doremalen N, Purushotham JN, Schulz JE, Holbrook MG, Bushmaker T, Carmody A, et al. Intranasal ChAdOx1 nCoV-19/AZD1222 vaccination reduces viral shedding after SARS-CoV-2 D614G challenge in preclinical models. Sci Transl Med 2021:13. https://doi.org/10.1126/SCITRANSLMED.ABH0755.
[69] Cao H, Mai J, Zhou Z, Li Z, Duan R, Watt J, et al. Intranasal HD-Ad vaccine protects the upper and lower respiratory tracts of hACE2 mice against SARS-CoV-2. Cell Biosci 2021:11. https://doi.org/10.1186/S13578-021-00723-0.
[70] Hassan AO, Kafai NM, Dmitriev IP, Fox JM, Smith BK, Harvey IB, et al. A single-dose intranasal ChAd vaccine protects upper and lower respiratory tracts against SARS-CoV-2. Cell 2020;183:169–184.e13. https://doi.org/10.1016/J.CELL.2020.08.026.

[71] Schultz MD, Suschak JJ, Botta D, Silva-Sanchez A, King RG, Detchemendy TW, et al. A single intranasal administration of AdCOVID protects against SARS-CoV-2 infection in the upper and lower respiratory tracts. Hum Vaccin Immunother 2022. https://doi.org/10.1080/21645515.2022.2127292.
[72] Szatmári T, Lumniczky K, Désaknai S, Trajcevski S, Hídvégi EJ, Hamada H, et al. Detailed characterization of the mouse glioma 261 tumor model for experimental glioblastoma therapy. Cancer Sci 2006;97:546–53. https://doi.org/10.1111/J.1349-7006.2006.00208.X.
[73] Fausther-Bovendo H, Kobinger GP. Pre-existing immunity against Ad vectors: Humoral, cellular, and innate response, what's important? Hum Vaccin Immunother 2014;10:2875. https://doi.org/10.4161/HV.29594.
[74] Mendonça SA, Lorincz R, Boucher P, Curiel DT. Adenoviral vector vaccine platforms in the SARS-CoV-2 pandemic. Npj Vaccines 2021 61 2021;6:1–14. doi: 10.1038/s41541-021-00356-x.
[75] An D, Li K, Rowe DK, Diaz MCH, Griffin EF, Beavis AC, et al. Protection of K18-hACE2 mice and ferrets against SARS-CoV-2 challenge by a single-dose mucosal immunization with a parainfluenza virus 5-based COVID-19 vaccine. Sci Adv 2021:7. https://doi.org/10.1126/SCIADV.ABI5246.
[76] Americo JL, Cotter CA, Earl PL, Liu R, Moss B. Intranasal inoculation of an MVA-based vaccine induces IgA and protects the respiratory tract of hACE2 mice from SARS-CoV-2 infection. Proc Natl Acad Sci USA 2022:119. https://doi.org/10.1073/PNAS.2202069119.
[77] Mathieu E, Ritchie H, Ortiz-Ospina E, Roser M, Hasell J, Appel C, et al. Coronavirus pandemic (COVID-19). Our World Data 2020;5:947–53. https://doi.org/10.1038/S41562-021-01122-8.
[78] Thangavel RR, Bouvier NM. Animal models for influenza virus pathogenesis, transmission, and immunology. J Immunol Methods 2014;410:60. https://doi.org/10.1016/J.JIM.2014.03.023.
[79] Neumann G, Watanabe T, Ito H, Watanabe S, Goto H, Gao P, et al. Generation of influenza A viruses entirely from cloned cDNAs. Proc Natl Acad Sci USA 1999;96:9345. https://doi.org/10.1073/PNAS.96.16.9345.
[80] Chen Z, Baz M, Lu J, Paskel M, Santos C, Subbarao K, et al. Development of a high-yield live attenuated H7N9 influenza virus vaccine that provides protection against homologous and heterologous H7 wild-type viruses in ferrets. J Virol 2014;88:7016. https://doi.org/10.1128/JVI.00100-14.
[81] Harding AT, Heaton BE, Dumm RE, Heaton NS. Rationally designed influenza virus vaccines that are antigenically stable during growth in eggs. MBio 2017:8. https://doi.org/10.1128/MBIO.00669-17.
[82] Breen M, Nogales A, Baker SF, Martínez-Sobrido L. Replication-Competent Influenza A Viruses Expressing Reporter Genes. Viruses 2016;8:1–28. https://doi.org/10.3390/V8070179.
[83] Fujii Y, Goto H, Watanabe T, Yoshida T, Kawaoka Y. Selective incorporation of influenza virus RNA segments into virions. Proc Natl Acad Sci USA 2003;100:2002. https://doi.org/10.1073/PNAS.0437772100.
[84] Lee KS, Wong TY, Russ BP, Horspool AM, Miller OA, Rader NA, et al. SARS-CoV-2 Delta variant induces enhanced pathology and inflammatory responses in K18-hACE2 mice. PLoS One 2022;17:e0273430.
[85] Barbier M, Lee KS, Vikharankar MS, Rajpathak SN, Kadam N, Wong TY, et al. Passive immunization with equine RBD-specific Fab protects K18-hACE2-mice against Alpha or Beta variants of SARS-CoV-2. Front Immunol 2022:13. https://doi.org/10.3389/FIMMU.2022.948431.
[86] Wong TY, Horspool AM, Russ BP, Ye C, Lee KS, Winters MT, et al. Evaluating antibody mediated protection against Alpha, Beta, and Delta SARS-CoV-2 variants of concern in K18-hACE2 transgenic mice 2022;96:2184–205. doi: 10.1128/JVI.02184-21.
[87] Lee KS, Russ BP, Wong TY, Horspool AM, Winters MT, Barbier M, et al. Obesity and metabolic dysfunction drive sex-associated differential disease profiles in hACE2-mice challenged with SARS-CoV-2. IScience 2022;25:105038. https://doi.org/10.1016/J.ISCI.2022.105038.
[88] Li D, Edwards RJ, Manne K, Martinez DR, Schäfer A, Alam SM, et al. The functions of SARS-CoV-2 neutralizing and infection-enhancing antibodies in vitro and in mice and nonhuman primates. BioRxiv 2021. https://doi.org/10.1101/2020.12.31.424729.
[89] Berry JD, Jones S, Drebot MA, Andonov A, Sabara M, Yuan XY, et al. Development and characterisation of neutralising monoclonal antibody to the SARS-coronavirus. J Virol Methods 2004;120:87. https://doi.org/10.1016/J.JVIROMET.2004.04.009.
[90] Coleman CM, Frieman MB. Growth and quantification of MERS-Cov Infection. Curr Protoc Microbiol 2015;37:1521. https://doi.org/10.1002/9780471729259.MC15E02S37.
[91] Kint J, Maier HJ, Jagt E. Quantification of infectious bronchitis coronavirus by titration in vitro and in ovo. Coronaviruses 2015;1282:89. https://doi.org/10.1007/978-1-4939-2438-7_9.